DNA Repair 14 (2014) 27–38

Contents lists available at ScienceDirect

DNA Repair

journal homepage: www.elsevier.com/locate/dnarepair

Gap-filling and bypass at the replication fork are both active mechanisms for tolerance of low-dose ultraviolet-induced DNA damage in the human genome

Annabel Quinet[a,b,*], Alexandre T. Vessoni[a], Clarissa R.R. Rocha[a], Vanesa Gottifredi[c], Denis Biard[d], Alain Sarasin[b], Carlos F.M. Menck[a,**], Anne Stary[b]

[a] Department of Microbiology, Institute of Biomedical Sciences, University of São Paulo, São Paulo, SP 05508-900, Brazil
[b] CNRS-UMR8200, Université Paris Sud, Institut de Cancérologie Gustave Roussy, 94805 Villejuif, France
[c] Fundación Instituto Leloir, CONICET, Buenos Aires, Argentina
[d] CEA, DSV-iMETI-SEPIA, BP6, 92265 Fontenay-aux-Roses, France

ARTICLE INFO

Article history:
Received 14 June 2013
Received in revised form
26 November 2013
Accepted 10 December 2013
Available online 28 December 2013

Keywords:
UV damage bypass
NER
TLS DNA polymerase η
Cell cycle progression
Replication fork
DNA strand breaks
γH2AX

ABSTRACT

Ultraviolet (UV)-induced DNA damage are removed by nucleotide excision repair (NER) or can be tolerated by specialized translesion synthesis (TLS) polymerases, such as Polη. TLS may act at stalled replication forks or through an S-phase independent gap-filling mechanism. After UVC irradiation, Polη-deficient (XP-V) human cells were arrested in early S-phase and exhibited both single-strand DNA (ssDNA) and prolonged replication fork stalling, as detected by DNA fiber assay. In contrast, NER deficiency in XP-C cells caused no apparent defect in S-phase progression despite the accumulation of ssDNA and a G2-phase arrest. These data indicate that while Polη is essential for DNA synthesis at ongoing damaged replication forks, NER deficiency might unmask the involvement of tolerance pathway through a gap-filling mechanism. ATR knock down by siRNA or caffeine addition provoked increased cell death in both XP-V and XP-C cells exposed to low-dose of UVC, underscoring the involvement of ATR/Chk1 pathway in both DNA damage tolerance mechanisms. We generated a unique human cell line deficient in XPC and Polη proteins, which exhibited both S- and G2-phase arrest after UVC irradiation, consistent with both single deficiencies. In these XP-C/Polη^{KD} cells, UVC-induced replicative intermediates may collapse into double-strand breaks, leading to cell death. In conclusion, both TLS at stalled replication forks and gap-filling are active mechanisms for the tolerance of UVC-induced DNA damage in human cells and the preference for one or another pathway depends on the cellular genotype.

© 2013 Elsevier B.V. All rights reserved.

1. Introduction

Ultraviolet (UV) light induces DNA damage that blocks replication and transcription [1–3] triggering either cell death or genetic instability. These lesions are removed through the nucleotide excision repair (NER) pathway which is defective in xeroderma pigmentosum (XP) syndrome characterized by UV hypersensitivity [2]. The NER pathway is subdivided into global genome repair (GG-NER) and transcription-coupled repair (TC-NER) [4]. Briefly, GG-NER removes lesions throughout the genome in a manner that depends on the XPC protein [3], whereas TC-NER targets lesions that stall RNA polymerase II. UV irradiation induces mainly (6-4) photoproducts (6-4PPs) and cyclobutane pyrimidine dimers (CPDs) in the DNA. Although 6-4PPs are formed 3 times less frequently than CPDs, they cause a more pronounced distortion in the DNA helix and are therefore more rapidly repaired by the GG-NER pathway (full removal within 3–6 h after irradiation). In contrast, only 60% of CPDs are excised within the first 24 h after UVC exposure in normal human cells [5,6].

Given the time required for full removal of UV-induced lesions, replication forks frequently encounter such distortions and processes that tolerate such replication barriers are activated. The most studied tolerance pathway in human cells is translesion DNA synthesis (TLS), a process involving specialized translesion polymerases capable of using damaged DNA as replicative templates [7]. Two models are currently proposed for TLS: at the blocked replication fork or via a post-replicative gap-filling mechanism

* Corresponding author. Present address: Department of Microbiology, University of São Paulo, São Paulo, SP 05508-900, Brazil. Tel.: +55 11 3091 7499; fax: +55 11 3091 7354.
** Corresponding author. Tel.: +55 11 3091 7499; fax: +55 11 3091 7354.
E-mail addresses: annabel.quinet@usp.br (A. Quinet), alexandre.vessoni@usp.br (A.T. Vessoni), calsmah@usp.br (C.R.R. Rocha), vgottifredi@leloir.org.ar (V. Gottifredi), denis.biard@cea.fr (D. Biard), sarasin@gustaveroussy.fr (A. Sarasin), cfmmenck@usp.br (C.F.M. Menck), stary@gustaveroussy.fr (A. Stary).

1568-7864/$ – see front matter © 2013 Elsevier B.V. All rights reserved.
http://dx.doi.org/10.1016/j.dnarep.2013.12.005

[8,9]. In the former, the stalled replicative polymerase is replaced by a TLS polymerase that inserts nucleotides opposite the lesion. The replicative polymerase is thereafter reassembled to allow the resumption of DNA replication following the lesion bypass. According to the second hypothesis, when encountering the lesions the replication forks are reinitiated after the damage, giving rise to single-stranded DNA (ssDNA) gaps opposite the lesions. In this scenario, fork progression should not directly depend on TLS, while TLS is in charge of filling ssDNA gaps [8,10–13] in a manner that is spatially and temporally dissociated from the replication fork [14–16]. If the ssDNA gaps are left unfilled, checkpoint signals are activated leading to a G2-phase cell cycle arrest [17–19].

DNA polymerase η (Polη, encoded by the *POLH* gene) is the prototypic TLS polymerase and the only TLS polymerase known which defects lead to a human syndrome [20], the variant form of XP (XP-V) [11]. It is well established that Polη ensures accurate replication of TT-CPDs [21,22] and this bypass may act at the stalled replication fork [23,24] but also through a post-replicative gap-filling pathway [15,25]. Polη may also be involved in the bypass of 6-4PPs as suggested by plasmids assays performed both in yeast and human cells [26,27]. However, Temviriyanukul and colleagues recently reported that Polη is mainly restricted to the TLS of CPDs, and they proposed that the bypass of 6-4PPs in the mammalian genome is performed by other TLS polymerases such as Rev1 and Polζ [24]. Therefore, the role of Polη in the TLS of 6-4PPs remains controversial.

In this work, we investigated the DNA damage response (DDR) in human cell lines deficient in GG-NER (XP-C cells) or Polη (XP-V cells) exposed to low-dose UVC irradiation. Indeed, we used a UVC dose that induced a mild sensitivity to both single-deficient cell lines but no detectable toxicity in wild-type cells (defined as low-dose UVC, in agreement with other authors, e.g. [28]). We analyzed the effects of UVC irradiation on the cell cycle progression, induction of DNA single- and double-strand breaks (DSBs) by alkaline and neutral comet assay, and the phosphorylation of the histone H2AX. Moreover, to gain further insights into the contribution of Polη in the DDR of XP-C cells to UVC exposure, we established a novel clonal human cell line stably knocked down (KD) for the *POLH* gene expression in an *XPC*-deficient background. Herein, we show that GG-NER- and/or Polη-deficient cells lines accumulate ssDNA after UVC irradiation, and cells lacking Polη arrest in early S-phase, while XP-C cells arrest in G2-phase. Importantly, upon UVC exposure, XP-V cells had a more pronounced replication fork stalling than DNA repair-deficient and control cells, and the KD of Polη in XP-C cells decreased fork elongation. Altogether, we report that according to the cellular genotype, both bypass at the replication fork and through a gap-filling pathway are active mechanisms that prevent the collapse of ssDNA into DSBs and ultimately cell death.

2. Material and methods

2.1. Cell culture and gene silencing

The SV40-transformed human fibroblasts XP4PA (XP-C), XP30RO (XP-V, kindly gifted by Dr. James Cleaver), MRC5, a NER-proficient clone derived from the XP4PA cell line, in which one copy of the causal *XPC* gene mutation has been corrected by homologous gene targeting, replaced by the *XPC* gene wild-type sequence (XP-C^{cor} cells, unpublished results) and XP-C/Polη^{KD} were routinely grown in DMEM (LGC) supplemented with 10% FCS (Cultilab) and 1% Penicillin/Streptomycin (Invitrogen, Life Technologies) at 37 °C in a humidified 5% CO_2 atmosphere. To stably switch off the *POLH* gene in XP-C human fibroblasts, Epstein–Barr-derived vectors carrying a short hairpin RNA (pEBVsiRNA) and a hygromycin B resistance gene were used as previously described [29–31]. The pEBVsiRNA vectors were transfected into XP-C cells using FugeneHD (Promega), and knock down (KD) populations and clones were selected and maintained in culture with 125 μg/mL of hygromycin B (Invitrogen, Life Technologies). We selected a clone that exhibited the most efficient gene silencing over time and termed it as XP-C/Polη^{KD} cells. XP-C/Polη^{KD} cells were cultivated for more than 30 passages, and gene silencing was regularly checked using western blotting. As controls, we used XP-C and XP-C^{cor} cells stably transfected with a pEBVsiRNA plasmid expressing an impaired shRNA sequence (shCTL) as previously mentioned [29]. All experiments were performed at the same time with XP-C/Polη^{KD}, XP-C shCTL and XP-C^{cor} shCTL cells. XP-C/Polη^{KD} cells were found to proliferate slower than their XP-C isogenic counterparts (Fig. S1), which is in agreement with previously reported data in U2OS cells that showed a Polη KD using the same pEBV-siRNA [30]. For transient depletion of ATR, 3×10^5 cells were plated in 60 mm dishes and were transfected, the next day, with 20 nM of specific small interfering RNA (siRNA) using Oligofectamine (Invitrogen, Life Technologies), according to the manufacturer's instruction. The following day, a second transfection was performed and 24 h later, cells were replated for subsequent experiments. The siRNA targeting ATR and the negative control sequences used were: ATR 5′-UUAACAUGUUCUUACCCUCAGGUGG-3′ (ATR-HSS100878 Stealth, Invitrogen, Life Technologies) [32] and control (CT) 5′-UUCUCCGAACGUGUCACGUdTdT-3′ (1027310, Qiagen). The human cells used in this work belong to a collection that has been approved by the Ethical Committee for Human Research at the University of São Paulo.

2.2. Ultraviolet irradiation

Exponentially growing cells were seeded 16 h prior to irradiation. For UVC irradiation, cells were washed with pre-heated phosphate buffer saline (PBS) and exposed to a germicide lamp (UVC, maximal emission at 254 nm). The UVC dose was monitored by a VLX-3W radiometer (Vilber Lourmat) and the rate used was 0.1 J/m^2/s. After the irradiation, cells received fresh medium and were incubated for the indicated times. For UVC irradiation concomitant with caffeine (Sigma–Aldrich) treatment, the drug was added in the complete culture medium at 1 mM final concentration caffeine (from a stock solution at 77.2 mM in PBS) after the UVC exposure.

2.3. Cell proliferation

Cell proliferation was assessed 72 h after UVC irradiation with or without caffeine using a Cell Proliferation Kit II (XTT, Roche) as described elsewhere [33]. Briefly, cells were seeded at 2×10^4 per well in a 12-well plate prior to treatment. 72 h after UVC irradiation, 400 μL of XTT labeling mixture was added to the cells and incubated for approximately 2 h at 37 °C. The absorbance was measured at 492 nm and 650 nm and the final result corresponds to the difference between these measures. Cell proliferation is expressed as percentage of unirradiated cells.

2.4. Flow cytometry (SubG1, γH2AX, active Caspase 3 and cell cycle analyses)

For concomitant SubG1 and γH2AX analyses, after the indicated recovery times, detached dying cells and trypsinized adherent cells were fixed with 1% formaldehyde in ice, washed with PBS, resuspended in 70% ice-cold ethanol and stored for at least 24 h at −20 °C. After blocking and permeabilization with BSA-T buffer (0.2% Triton X-100, Sigma–Aldrich, 1% bovine serum albumin,

BSA, Sigma–Aldrich, in PBS), samples were incubated with 1/500 anti-γH2AX antibody (05-636 Millipore) overnight at 4 °C or for 3 h at room temperature (RT). Samples were then washed twice with BSA-T buffer and incubated with 1/200 anti-mouse fluorescein iso-thiocyanate (FITC) antibody (Sigma–Aldrich) for 1 h at RT in the dark. After two washings, the DNA content was stained with 20 μg/mL propidium iodide (PI), 200 μg/mL de RNase A (Invitrogen, Life Technologies) and 0.1% Triton X-100 in filtered PBS for 40 min at RT. We defined a gate for γH2AX positive cells based on unirradiated cells that were considered negative to this staining. To detect and quantify the formation of the active form of Caspase 3, the immunostaining was performed at RT for 1 h and 30 min using a FITC-conjugated anti-active Caspase 3 antibody (559341 BD Pharmigen) diluted at 1/10. To study the cell cycle, cells were treated, let recover for the indicated times and labeled with 10 μM of bromodeoxyuridine (BrdU, Sigma–Aldrich), a thymidine analog, for 20 min prior to harvesting. Cells were then detached, washed twice with PBS, fixed with 75% chilled ethanol and stored at −20 °C. The day before the acquisition, DNA was treated with pepsin (14 μM, 1.5% HCl 2 M in water, 250 U/mg, Sigma–Aldrich) for 20 min at 37 °C and then with HCl 2 M for 20 min at RT. Cells were then washed with PBS and blocked and permeabilized with Bu buffer (0.5% FBS, 0.5% Tween-20, 20 mM Hepes in PBS), before incubation with 1/100 anti-BrdU (mouse, Invitrogen, Life Technologies) for 1 h. Samples were then washed and incubated 45 min at the dark in 1/200 anti-mouse FITC (Sigma–Aldrich). Finally, DNA was stained with PI as described above. We defined gates for G1-, S- and G2-phases based on BrdU and DNA content staining. G1- and G2-phase cells are BrdU negative, in contrast to S-phase cells that are BrdU positive. G2-phase cells present twice DNA content than G1-phase cells. Samples were applied on a Guava Flow Cytometer (Millipore) and the data analyzed with CytoSoft Data Acquisition and Analysis Software (Millipore). For SubG1 and γH2AX analyses, 10,000 cells were counted for each sample and 5000 cells were acquired for cell cycle.

2.5. Immunofluorescence

For local UVC irradiation, cells were covered with a 5 μm pore-diameter filter (Millipore) during exposure, and immunostaining was subsequently performed as previously described [34] with the following antibodies: rabbit anti-γH2AX (ab-2893 Abcam) at 1/100 and mouse anti-RPA p34 (MS-691-P0 Neomarkers) at 1/2000. For ssDNA staining, cells were cultivated in the presence of BrdU for 48 h (two doubling times) before UVC exposure. Cells were then immunostained with a mouse anti-BrdU (347580 BD Biosciences) at 1/50 and a rabbit anti-Cyclin A (sc-751 Santa Cruz) antibody at 1/100 in non denaturing conditions. The secondary antibodies used were anti-mouse Alexa Fluor 594 and anti-rabbit Alexa Fluor 488 (Invitrogen, Life Technologies). Slides were imaged with a fluorescence microscope (Axiovert 200, Zeiss) at a magnification of 1000×.

2.6. DNA fiber assay

The analyses of replication forks progression after UVC irradiation were performed as previously described [35]. Briefly, 3×10^5 cells were seeded in 35 mm plates. The next day, cells were pulsed with 20 μM chlorodeoxyuridine (CldU, Sigma–Aldrich), a thymidine analog, for 20 min, washed twice with PBS, irradiated with 20 J/m^2 UVC (or non irradiated as control), then incubated with 200 μM of another thymidine analog, Iododeoxyuridine (IdU, Sigma–Aldrich), for 20 or 60 min. Cells were then trypsinized and resuspended in PBS for final concentration of 1250 cells/μl. A total of 2.5×10^3 cells were placed onto glass slide and lysed with 6 μl of 0.5% SDS, 200 mM Tris-HCl (pH 7.4) and 50 mM EDTA. To unwind DNA, slides were tilted allowing a stream of DNA to run slowly down the slide. Then, slides were fixed in methanol-acetic acid (3:1) and kept overnight in ethanol 70% at 4 °C. The samples were then denatured (2.5 M HCl for 1 h) and blocked in BSA 5%. IdU incorporation was detected using mouse anti-BrdU (1/40, BD Biosciences) and anti-mouse Alexa Fluor 594 secondary antibody. Rat anti-BrdU (1/40, Accurate Chemicals) and anti-rat FITC secondary antibody were used for CldU detection. Finally, slides were mounted with Fluoroshield (Sigma–Aldrich) and DNA fibers were image using confocal microscopy (Zeiss LSM-780 NLO). The lengths of DNA tracts were analyzed by using Zeiss LSM Image Browser software. The experiments were performed twice independently and at least 100 fibers were measure for each sample.

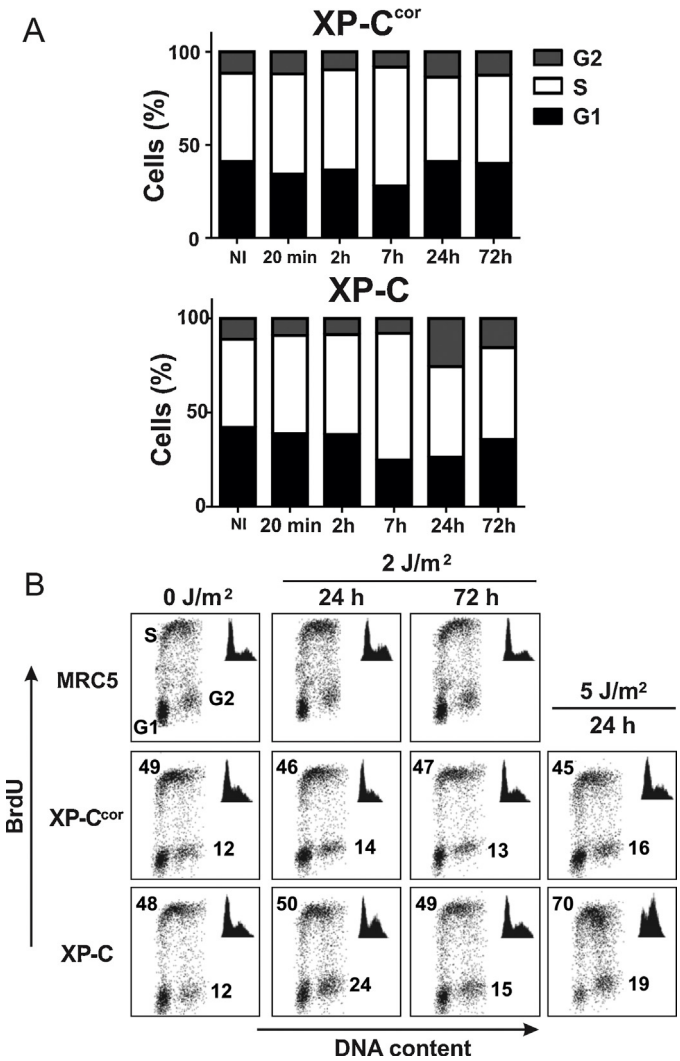

Fig. 1. XP-C cells temporarily accumulate in the G2-phase of the cell cycle after a low UVC dose exposure. The cell cycle phases distribution of wild-type and XP-C cells after 2 J/m^2 UVC was evaluated by BrdU and propidium iodide (PI) staining and was detected by flow cytometry. Briefly, S-phase cells are BrdU positive, while G1 and G2-phase cells are negative for BrdU. PI, a DNA intercalating agent, indicates that G2-phase cells contain two-fold more DNA content than G1-phase cells. (A) Quantification of the flow cytometry data showing the percentage of cells in each cell cycle phase at the indicated times after a 2 J/m^2 UVC dose. At least two independent flow cytometry experiments were performed in duplicate. (B) Representative graphics are shown and the average percentages of cells in G1-, S- and G2-phases obtained via three independent experiments are indicated. At the top right, the corresponding cell cycle distributions determined by PI staining are shown.

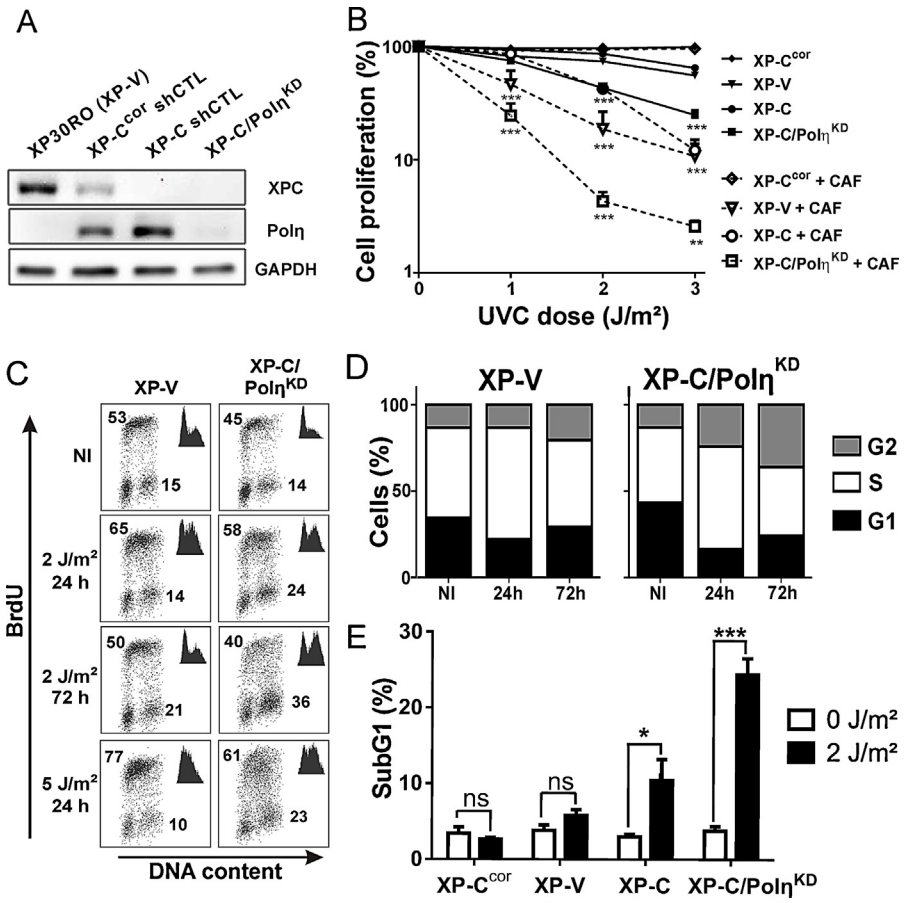

Fig. 2. XP-C/Polη^{KD} cells present both XP-C and XP-V phenotypes and are more sensitive to low-dose UVC irradiation than XP-C cells. (A) *POLH* was stably knocked down in XP-C human fibroblasts as assessed by western blotting. (B) The proliferation of XP-C^{cor}, XP-V, XP-C and XP-C/Polη^{KD} cells was determined 72 h after 0, 1, 2 and 3 J/m^2 doses of UVC with or without 1 mM caffeine (CAF). The significance of the difference between each cell line irradiated with 2 J/m^2 UVC without CAF compared to UVC + CAF was determined by Two-way ANOVA (**$P < 0.01$; ***$P < 0.001$). (C) The cell cycle phases of XP-V and XP-C/Polη^{KD} cells were evaluated by BrdU and DNA content (PI) staining as detected by flow cytometry at the indicated times after UVC treatment. Representative graphics are shown, and the averages of the percentages of cells in G1-, S- and G2-phases from three independent experiments are indicated. At the top right, the cell cycle distribution determined by PI staining is shown. (D) Averages of the percentages of cells in each cell cycle phase from three independent flow cytometry experiments. (E) SubG1 fractions were detected by flow cytometry 72 h after treatment. Each value represents the mean (±s.e.m.) of at least three independent experiments. The significance of the differences between 0 and 2 J/m^2 for each cell line was evaluated with unpaired *t*-test (ns, non significant, *$P < 0.05$; ***$P < 0.001$).

2.7. Western blot

The detection of endogenous proteins was performed as previously described [23]. The following antibodies were used: rabbit anti-Polη (ab-17725 Abcam), mouse anti-XPC (ab-6264 Abcam), rabbit anti-p-Chk1 Ser345 (2348 Cell Signaling) and mouse anti-GAPDH (sc-32233 Santa Cruz).

2.8. Alkaline and neutral comet assays

To detect DNA strand breaks, either immediately or 24 h after treatment, 10^5 cells, seeded in 35 mm plates, were trypsinized and resuspended in 180 μL of 0.5% low melting point (LMP) agarose at 37 °C. Cells were then homogenously spread onto two microscope slides precoated with 1.5% agarose and were immediately covered with coverslips. To solidify the LMP agarose, the slides were kept at 4 °C for 10 min. After carefully removing the coverslips, cells were lysed overnight in chilled lysis solution (2.5 M NaCl, 100 mM EDTA, 10 mM Tris and freshly added 1% Triton X-100 and 10% dimethyl sulfoxide (DMSO) pH 10) at 4 °C. The slides were then placed horizontally in an electrophoresis chamber with cold alkaline buffer (300 mM NaOH, 1 mM EDTA, pH >13) for 25 min, and electrophoresis was performed for 25 min at 25 V and 300 mA. For the neutral comet assay, after the overnight lysis, the slides were washed three times with chilled neutral electrophoresis buffer (300 mM sodium acetate, 100 mM Tris, acetic acid, pH 8.5) and equilibrated for 1 h horizontally in this cold buffer before being subjected to electrophoresis for 1 h at 14 V and 12 mA. Subsequently, slides were neutralized with three 5-min washes with neutralization buffer (0.4 M Tris, pH 7.5) and fixed with ice-cold 100% ethanol. Finally, the slides were stained with ethidium bromide and imaged with a fluorescence microscope (Axiovert 200, Zeiss) at a magnification of 400×. At least 100 comets per slide were scored with the Comet Assay IV software (Perceptive Instruments).

2.9. Statistical analysis

Statistical significance was assessed using unpaired test, one-way ANOVA or two-way ANOVA followed by the Bonferroni test (Prism 5, GraphPad Software Inc.).

3. Results

3.1. XP-C human cells temporarily accumulate in G2-phase after low-dose UVC irradiation

To study the DDR in GG-NER-deficient cells, the effects of UVC irradiation on XP-C fibroblasts were investigated and compared to

the isogenic cell line corrected for the expression of a wild-type XPC protein (XP-C^{cor} cells) as described in Section 2. First, we used a "low UVC dose" (2 J/m^2) that we defined as a UVC dose that does not induce any detectable sensitivity in XP-C^{cor} cells and only a mild effect on XP-C cells (70% of cell proliferation compared to untreated XP-C cells, Fig. S2). Flow cytometry analysis showed that 7 h after 2 J/m^2, the percentage of S-phase cells increased in both XP-C and XP-C^{cor} fibroblasts (Fig. 1A). At later time, this S-phase accumulation was no longer detected in both cell lines. In fact, 24 h after treatment, despite resumption of a normal cell cycle progression in NER-proficient cells, we detected a two-fold increase in the number of XP-C fibroblasts in G2-phase relative to control cells (Fig. 1). This accumulation of XP-C cells in G2-phase was less pronounced 72 h after UVC exposure, although it did not return to basal levels. Interestingly, 24 h after irradiation, DNA replication proceeded normally in XP-C cells, as evidenced by no decrease in either BrdU incorporation or cell accumulation in S-phase (Fig. 1B). Moreover, following a higher UVC dose irradiation (5 J/m^2), XP-C cells accumulated in both late S- and G2-phases, unlike NER-proficient cells (Fig. 1B). This suggests that defects in GG-NER might impair events required for the completion of S-phase after UVC irradiation, leading to a G2-phase accumulation.

3.2. Deficiency in both XPC and Polη proteins triggers accumulation in S- and G2-phases after low-dose UVC irradiation

We next sought to determine the role of Polη in low-dose UVC-irradiated human cells deficient in GG-NER. Polη was stably knocked down (Polη^{KD}) in XP-C fibroblasts using a pEBVsiRNA vector targeting the *POLH* gene [30,36]. From transfected cells, the clone with the highest KD efficiency and nearly undetectable Polη protein level was selected and named XP-C/Polη^{KD} (Fig. 2A). Because UVC sensitization by caffeine (CAF) is a hallmark of the XP-V cell phenotype [11,22,37], we characterized the Polη KD phenotype through its sensitivity to UVC irradiation in the presence of 1 mM CAF (Fig. 2B). Although the proliferation of XP-C^{cor} fibroblasts after UVC treatment was not affected by this drug, XP-C, XP-V and XP-C/Polη^{KD} fibroblasts displayed a strong decreased proliferation after combined UVC irradiation (2 and 3 J/m^2) and CAF treatment (Fig. 2B). Importantly, consistent with the defect of Polη, only XP-V and XP-C/Polη^{KD} cells were sensitized by CAF with an irradiation as low as 1 J/m^2 UVC. Strikingly, after 2 J/m^2 UVC dose, the proliferation rate of fibroblasts was disrupted to a greater extent in the XP-C/Polη^{KD} cells as compared to their isogenic XP-C counterparts, even in the absence of CAF (Fig. 2B and Fig. S2). This result highlighted the crucial contribution of Polη deficiency toward the sensitivity of XP-C cells to UVC irradiation. To better characterize the low-dose UVC-induced DDR in this double-deficient cell line, the cell cycle and SubG1-phase were analyzed by flow cytometry (Fig. 2C, D and E). At 24 h post 2 J/m^2, while XP-C and XP-V cells accumulated in G2 and early S-phase, respectively (compare Figs. 1B and 2C), XP-C/Polη^{KD} fibroblasts accumulated in both G2- and S-phases. At 72 h, BrdU incorporation assay showed a clear disrupted S- to G2-phase transition in XP-C/Polη^{KD} cells, and a greater accumulation of cells in G2-phase than that observed 24 h after UVC (36% compared to 24%). It is noteworthy that irradiated XP-V cells moderately accumulated in G2-phase (21%, Fig. 2C) at this time point. Besides, XP-C/Polη^{KD} cells exhibited an increased SubG1 fraction (24%) as compared to XP-V cells (5.8%) and XP-C cells (10.5%, Fig. 2E).

While at a dose of 5 J/m^2 UVC, XP-V cells accumulated in early S-phase, to a greater extent than that observed at 2 J/m^2 (77% versus 65% respectively) (Fig. 2C), XP-C/Polη^{KD} cells exhibited a robust impairment in the amount of BrdU incorporation, indicating a strong defect in the ability to maintain active fork progression in cells transiting S-phase (also shown in the cell cycle profile

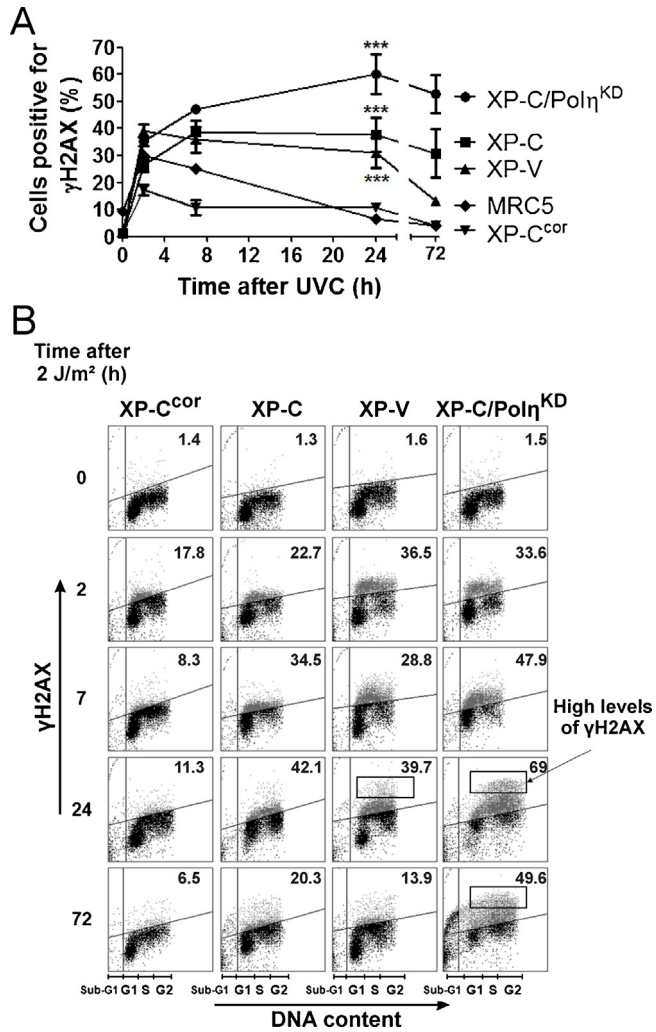

Fig. 3. NER- and Polη-deficient cells present persistent γH2AX formation upon a low UVC dose. (A) γH2AX immunostaining was detected by flow cytometry at the indicated times after a 2 J/m^2 UVC dose. Cells showing a more intense γH2AX signal than untreated cells were considered positive. Data are shown as the mean (± s.e.m.) of percentages of γH2AX-positive cells excluding cells in the SubG1 fraction from three independent experiments. The significance of the differences between XP-C/Polη^{KD} cells versus XP-C cells and between XP-C and XP-V cells versus MRC5 cells were evaluated by Two-way ANOVA (***$P < 0.001$). (B) Histograms show representative γH2AX staining as a function of DNA content at the indicated times after 2 J/m^2 UVC. The percentages of γH2AX-positive cells (including SubG1 cells) are indicated at the top right of each panel. G1-, S-, G2-phases and SubG1 fraction are shown and the rectangles indicate cells with a more intense and distinguishable γH2AX staining, defined as high levels of γH2AX.

inset in the upper corner of the panels). Altogether, these results indicate that human fibroblasts deficient in both XPC and Polη proteins exhibited the combined XP-C and XP-V phenotypes and were extremely sensitive to low-dose UVC irradiation.

3.3. Persistent H2AX phosphorylation in XP-V, XP-C and XP-C/Polη^{KD} human cells exposed to low-dose UVC

The variant histone H2AX is phosphorylated at serine 139 (forming γH2AX) in the vicinity of single-stranded DNA (ssDNA), DNA single- or double-strand breaks (SSBs and DSBs, respectively) [38–40]. Because UVC irradiation induces γH2AX formation [39–43], this was investigated in NER- and/or Polη-deficient human cells. Firstly, we sought to study the formation of γH2AX in spatially restricted UVC-irradiated sites within the nuclei by irradiating cells with 150 J/m^2 UVC through 5-μm diameter isopore

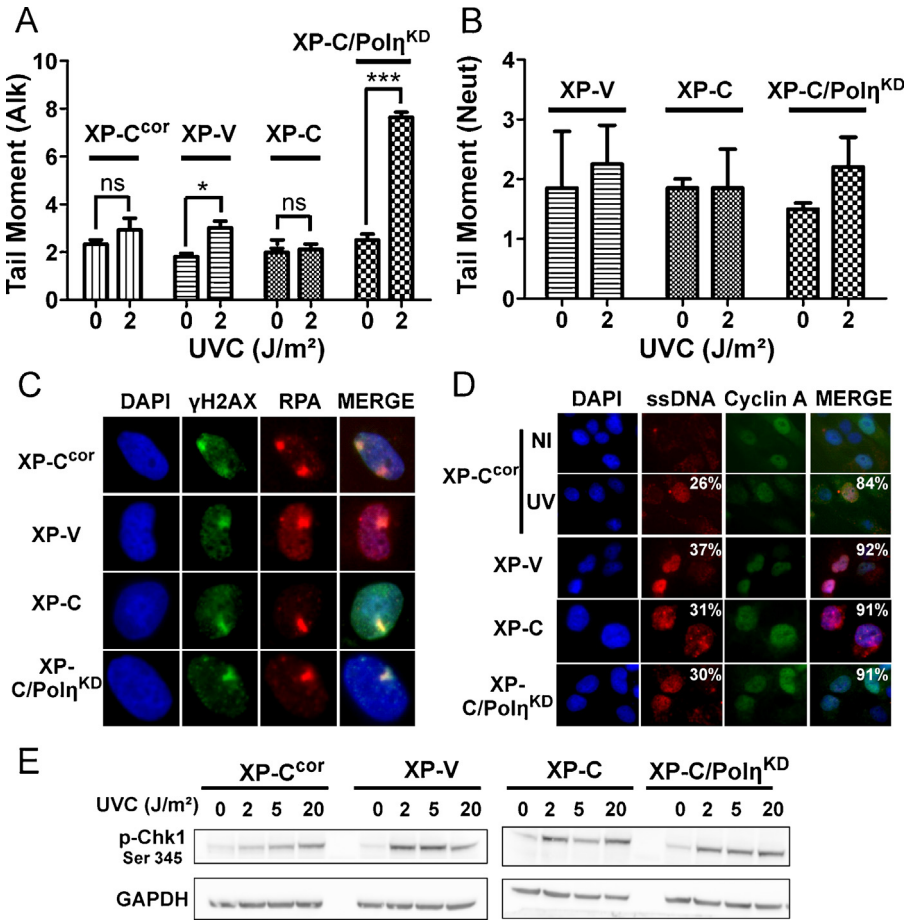

Fig. 4. Polη-deficient cells exhibit single-strand breaks and single-strand DNA while XP-C cells only present single-strand DNA. DNA strand breaks (single-strand breaks, SSB and double-strand breaks, DSB) (A) and only DSB (B) were detected 24 h after UVC treatment using the alkaline (Alk) and neutral (Neut) comet assay, respectively. Data are presented as means of comet tail moment (±s.e.m.) from at least two experiments performed in triplicate; 100 comets per sample were scored. Statistical analyses were applied by comparing treated versus untreated cells with unpaired *t*-test. (ns, non significant; $^{*}P < 0.05$; $^{***}P < 0.001$). (C) Cells were exposed to a 150 J/m^2 UVC dose through 5 μm-diameter isopore filters and were immunostained for γH2AX and RPA p34 7 h later. (D) Cells incorporated BrdU for 48 h and were co-immunostained 6 h after 20 J/m^2 in non denaturing conditions for Cyclin A and BrdU, revealing the presence of single-strand DNA (ssDNA) in S/G2-phase cells. The percentages of ssDNA-positive cells are indicated in the ssDNA panels and the percentages of ssDNA-positive cells that were also positive for Cyclin A are shown in the Merge panel. At least 100 nuclei were scored per condition. (E) The phosphorylated form of Checkpoint 1 at Serine 345 (p-Chk1) was detected by western blotting 6 h after the indicated UVC doses.

filters. Immediately after local irradiation, no γH2AX staining was detected, although signals specific to CPD photoproducts were intense (Fig. S3). At later time points after UVC irradiation (2 and 7 h), γH2AX staining reached strong intensities in areas containing CPDs and 6-4PPs in both NER-proficient and deficient cell lines. Next, we assessed the phosphorylation of H2AX after low UVC dose exposure (Fig. 3). In agreement with the local UVC irradiation experiments, flow cytometry analysis showed that immediately after exposure to 2 J/m^2 UVC there was no γH2AX formation in any cell lines (Fig. 3A). While at 2 h after irradiation γH2AX staining increased in all cell lines, 24 h later γH2AX was no longer detected in XP-C^{cor} cells. In contrast, a strong accumulation of γH2AX-positive XP-V (31%) and XP-C (38%) cells was observed. Moreover, at that time XP-C/Polη^{KD} cells exhibited two fold more γH2AX-positive cells than XP-C and XP-V fibroblasts (Fig. 3A). A slight decrease in γH2AX staining intensity was detected in the two NER-deficient cell lines 72 h after UVC treatment. In the NER-proficient XP-V cells, this decrease was more evident, although it did not return to its basal level. These data suggest that H2AX is phosphorylated as a consequence of the persistence of unrepaired photoproducts in the genome.

To gain further insights into the formation of γH2AX in these deficient cell lines, we analyzed the γH2AX signal as a function of the DNA content as shown by propidium iodide staining (Fig. 3B). In all deficient cell lines, the formation of γH2AX was observed in all cell cycle phases, although the staining appeared in an arc-form, revealing a more pronounced signal mainly in S-phase. Interestingly, a more intense γH2AX staining, distinguishable from the staining exhibited by the majority of cells, (see Fig. 3B, indicated as high levels of γH2AX), was detected in S- and G2-phase XP-V and XP-C/Polη^{KD} cells 24 h after UVC, which was persistent and much more pronounced in the double-deficient cell line.

3.4. Low-dose UVC induces ssDNA in XP-V, XP-C and XP-C/Polη^{KD} cells, while SSBs are detected only in Polη-deficient cells

The relevance of γH2AX staining as a witness of DNA strand breaks was assessed by the alkaline comet assay, which detects both SSB and DSB. Importantly, no DNA strand breaks were detected immediately after UVC exposure, indicating that they are not directly induced by this irradiation (Fig. S4). Surprisingly, 24 h after 2 J/m^2 UVC, when γH2AX staining was at a maximum for all the three deficient cell lines, DNA strand breaks were significantly induced only in Polη-deficient cell lines (XP-V and XP-C/Polη^{KD} cells) but not in the XP-C fibroblasts (Fig. 4A). To distinguish between SSBs and DSBs, we next assessed DSB formation using the neutral comet assay (Fig. 4B). We did not detect a significant induction of DSBs in any of the three deficient cell lines, although

there was a slight increase of DSBs in XP-V and XP-C/Polη^{KD} cells (Fig. 4B and Fig. S5). Thus, a low UVC dose induced mainly SSBs in both XP-V and XP-C/Polη^{KD} cells, although they were two-fold more pronounced in the double-deficient cell line. Interestingly, the representation of tail moment as a function of DNA content indicates that under alkaline conditions DNA strand breaks are formed during the S-phase of XP-V and XP-C/Polη^{KD} cells (Fig. S5), which is in agreement with the γH2AX staining detected predominantly in S-phase cells.

Previous work has shown that UVC-induced γH2AX formation was linked to the presence of ssDNA [40,42,44]. Moreover, it has been shown that ssDNA can be detected as SSB by the alkaline comet assay [39,45]. To investigate if SSBs result from ssDNA in replicating DNA, we used local UVC irradiation with immunofluorescence to follow the co-localization of γH2AX with replication protein A (RPA), a protein that binds ssDNA, and is therefore widely used as an ssDNA marker. Strikingly, γH2AX and RPA co-localized in all cell lines 7 h after local UVC treatment (Fig. 4C). However, we cannot exclude that the high UV dose, employed for local UV, may also induce the formation of DSBs. As a further assay, the presence of ssDNA was also investigated by labeling both DNA strands with a thymidine analog, BrdU, for 48 h and subsequent BrdU immunostaining in non denaturing conditions 6 h after 20 J/m^2 of UVC (Fig. 4D). In these conditions, BrdU antibody identifies only single-stranded molecules, staining the cells when ssDNA are present. The formation of ssDNA was observed in all cell lines only after UVC-irradiation of the cells. The results show that, following 20 J/m^2, deficient cell lines presented slightly more ssDNA than XP-C^{cor} cells, and also that, for the three deficient cell lines, the large majority (more than 90%) of the ssDNA-positive cells were also stained positive for Cyclin A, a protein that is expressed during S- and G2-phases [46].

The formation of ssDNA was shown to activate the Ataxia Telangiectasia and Rad-3 related (ATR) pathway [23,24], thus we investigated, in these cells, the phosphorylation at Serine 345 of Checkpoint 1 (Chk1), a downstream target for the ATR kinase (Fig. 4E). Indeed, 6 h after 2, 5 and 20 J/m^2 UVC, all cell lines exhibited phosphorylated Chk1 (p-Chk1). Interestingly, after 2 J/m^2 UVC, XP-C, XP-V and XP-C/Polη^{KD} cells showed similar and pronounced levels of p-Chk1 when compared to XPC^{cor} cells.

In summary, the different cell cycle progression defects resulting from XPC or Polη deficiency are both associated with ssDNA accumulation and γH2AX formation after low doses of UVC.

3.5. UVC irradiation induces a pronounced stalling of replication forks in Polη-deficient cells

Considering that (i) low-dose UVC irradiated XP-V and XP-C/Polη^{KD} cells were arrested in the S-phase of cell cycle, while XP-C cells exhibited a G2-phase arrest (Figs. 1 and 2C and D), and (ii) in all these three cell lines low UVC doses induced ssDNA (Fig. 4), we hypothesized that the lack of Polη would lead to the stall of replication forks at the DNA damage, while deficiency of XPC protein would lead to gap formation, with no replication fork stalling. To address this question, replication fork elongation was assessed using the DNA stretching technology (fiber assay) for all cell lines, 20 or 60 min after irradiation with 20 J/m^2 (Fig. 5). Briefly, two thymidine analogs were incorporated in nascent DNA strand during an initial 20 min pulse (CldU) and a subsequential pulse (IdU) of 20 or 60 min after UVC irradiation (Fig. 5A). In the first settings (20 min CldU/20 min IdU), a CldU/IdU ratio of 1 is expected in the absence of replication fork arrest, and a value higher than 1 indicates the stalling of the nascent DNA fibers at the damage. In the second settings (60 min IdU pulse), a smaller ratio of 0.33 is expected in the absence of arrest. With an IdU pulse of 20 min, irradiated XP-C

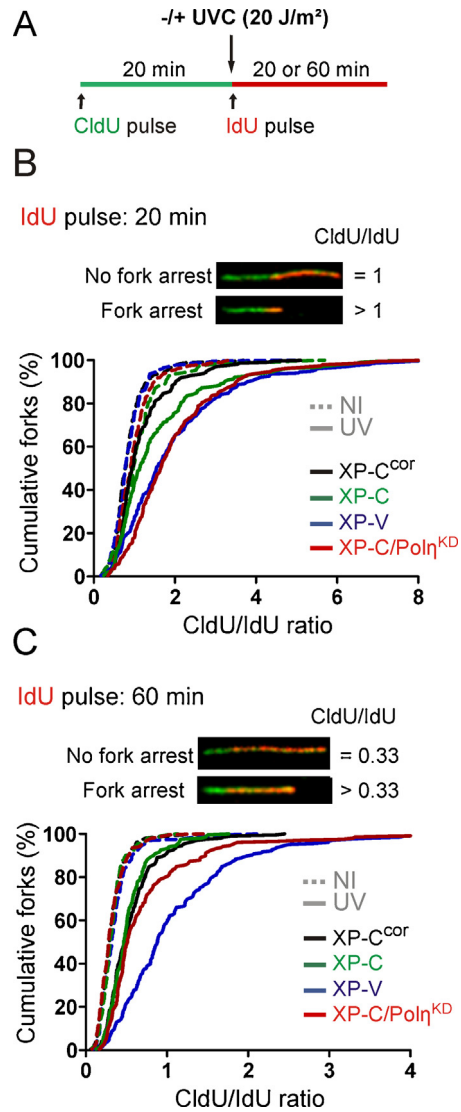

Fig. 5. UVC irradiation stalls replication forks in Polη-deficient cells in a more pronounced way than in XP-C and XP-C^{cor} cells. (A) Scheme of the DNA fiber experiment. Cumulative frequency distribution of CldU/IdU ratio expressed as percentage of cumulative forks for fibroblasts irradiated with 20 J/m^2 (UV) or non irradiated (NI) and pulsed with IdU for 20 min (B) or 60 min (C) from two independent experiments; at least 100 fibers per sample were scored.

cells exhibited a slightly increased CldU/IdU ratio when compared to XP-C^{cor} cells, although at 60 min this difference was abolished (Fig. 5B and C). In contrast, XP-V and XP-C/Polη^{KD} cells exhibited a more pronounced replication fork stalling than XP-C and XP-C^{cor} cells (indicated by a CldU/IdU ratio increase) (Fig. 5B and C) at both 20 and 60 min after UVC. It is noteworthy that XP-C/Polη^{KD} cells seem to exhibit the shortest CldU track length among all cell lines (Fig. S6), in agreement with the slow growth upon KD of Polη in XP-C cells (Fig. S1).

3.6. Caffeine highly sensitizes GG-NER-deficient cells exposed to low-dose UVC irradiation

The effect of CAF on the proliferation of XP-C cells exposed to 2 J/m^2 of UVC was unexpected (Fig. 2B). We therefore investigated the effects of CAF on cell cycle progression using quantitative flow cytometry experiments. Such assays revealed that upon CAF treatment irradiated XP-V cells clearly accumulated in early S-phase (Fig. 6A), while XP-C cells accumulated in both S- and

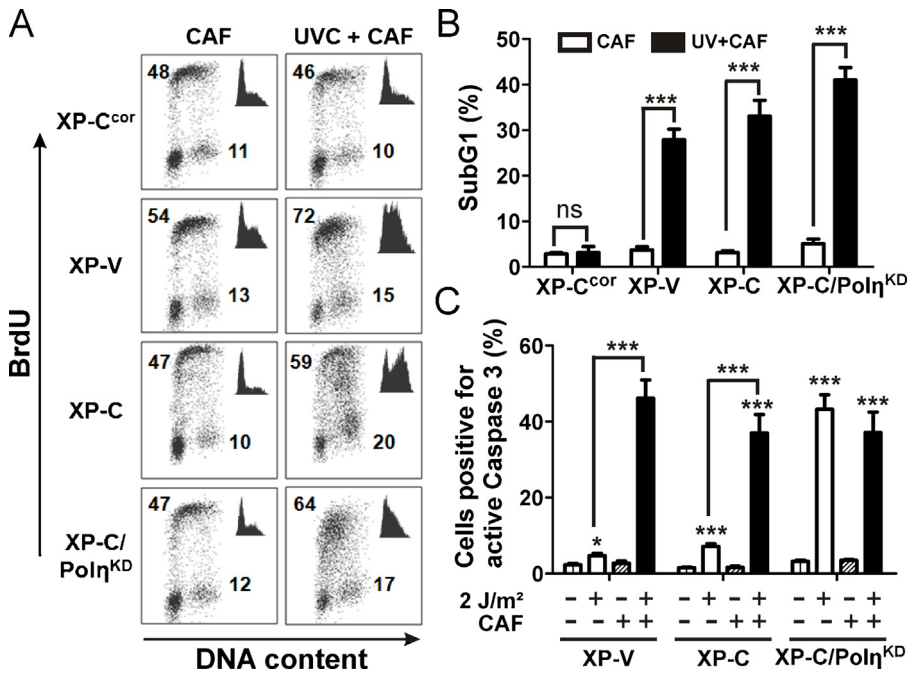

Fig. 6. UVC-irradiated Polη-deficient and GG-NER-deficient cells are highly sensitized by caffeine. Cells were treated with 2 J/m^2 UVC in the presence of 1 mM of caffeine (CAF). (A) Cell cycle progression was assessed 24 h after treatment by co-staining cells with anti-BrdU and propidium iodide (PI) followed by flow cytometry analysis. At the top right, the correspondent cell cycle distribution determined only by PI staining is shown. Flow cytometry analyses were done at least three times independently in duplicate. Representative graphics are shown and the averages of the percentages of cells in G1-, S- and G2-phases from three individual experiments are indicated. (B) The SubG1 fraction was detected by flow cytometry 72 h after the exposure. Each value represents the mean (±s.e.m.) of at least three independent experiments. The significance of the differences between CAF only versus UVC + CAF were evaluated for each cell line with unpaired *t*-test (ns, non significant, ***$P < 0.001$). (C) The formation of the active form of Caspase 3 was quantified by flow cytometry 72 h after the indicated treatments. Data correspond to the means (±s.e.m.) of three independent experiments. Statistical analyses between 0 and 2 J/m^2 for each cell line were performed with unpaired *t*-test, while those between irradiated cells treated or not with CAF were done with One-way ANOVA (*$P < 0.05$; ***$P < 0.001$).

G2-phases. Finally, XP-C/Polη^{KD} fibroblasts subjected to combined UVC and CAF treatments showed steep accumulation in S-phase with decreased BrdU incorporation (Fig. 6A). Moreover, CAF induced an increase in SubG1 cells in all irradiated deficient cell lines, correlating with the increase in cell sensitivity to UVC irradiation (Fig. 6B). Indeed, 72 h after this concomitant treatment, XP-V and XP-C cells presented 28% and 33% of SubG1 fraction, respectively, and 41% of XP-C/Polη^{KD} cells were observed in the SubG1 fraction at this time point (Fig. 6B). To gain further insights into the mechanisms of low-dose UVC and CAF-induced cell death in these deficient cell lines, active Caspase 3-positive cells were quantified by flow cytometry, indicating apoptosis (Fig. 6C). UVC significantly increased the percentage of active Caspase 3-positive cells in XP-V (5%), XP-C (7%) and XP-C/Polη^{KD} (43%). CAF highly sensitized XP-V (46%) and XP-C (37%) cells to UVC, while the levels of active Caspase 3 remained high in XP-C/Polη^{KD} cells. Therefore, CAF impaired DNA replication (measured by BrdU incorporation) and resulted in cell death by apoptosis (revealed by DNA fragmentation and Caspase 3 activation) in XP-V, XP-C and XP-C/Polη^{KD} human cells irradiated with low UVC dose.

3.7. *Caffeine induces high levels of γH2AX and DNA double-strand breaks in XPC- and Polη-deficient fibroblasts after a low UVC dose exposure*

To further investigate the mechanism by which UVC and CAF sensitized XP-C, XP-V and XP-C/Polη^{KD} fibroblasts, we studied the phosphorylation of H2AX and the formation of SSB and DSB by comet assay (Fig. 7). CAF did not increase UVC-induced γH2AX in XP-C^{cor} cells at any time analyzed (Fig. S7), while all deficient cell lines showed a more pronounced accumulation of γH2AX 24 h after this co-treatment. Furthermore, flow cytometry analysis showed that CAF increased the number of cells with intense γH2AX staining, which was particularly evident at longer time points (24 and 72 h, Fig. S8). Importantly as well, CAF led to an increase on the amount of cells presenting an intense pan-nuclear γH2AX staining in UVC-irradiated XP-C/Polη^{KD} cells detected by immunofluorescence (Fig. S9), similar to the γH2AX staining in human fibroblasts exposed to 20 J/m^2 UVC previously reported by Cleaver et al. [42,47]. These observations support that, in our study, cells presenting intense γH2AX staining in flow cytometry assays correspond to cells with "high levels of γH2AX" as defined by Cleaver's group [47].

We also classified γH2AX staining as "moderate" or "high" (Fig. S8). The CAF-induced increase in the percentage of γH2AX-positive cells was caused mainly by an increase in the cell population with high levels of γH2AX (Fig. 7A). These cells were predominantly observed in S- and G2-phases of cell cycle (Fig. S8). Strikingly, CAF also increased UVC-induced DNA breaks in XP-V and XP-C/Polη^{KD} cells 24 h after treatment (Fig. 7B). Indeed, CAF treatment induced (in XP-C cells) or amplified (in XP-V or XP-C/Polη^{KD} cells) the tail moment in UVC-irradiated cells as compared to cells treated with UVC only (compare Figs. 7B and 4A). CAF also generated DSBs in all deficient cell lines (Fig. 7C and S10), which were only barely detected in UVC-exposed cells in the absence of CAF (Fig. 4C). Together, the data show that CAF enhanced UVC-induced DNA replication arrest, production of DSBs and high levels of γH2AX in both XP-V and XP-C/Polη^{KD} cells. In irradiated XP-C cells, on the other hand, S-phase stalling, high levels of γH2AX and DNA breaks appeared only in the presence of CAF.

3.8. *ATR inhibition yields DNA damage effects similar to caffeine*

Previous work has suggested that the effects of CAF in UVC-exposed human cells are due to the inhibition of the ATR/Chk1

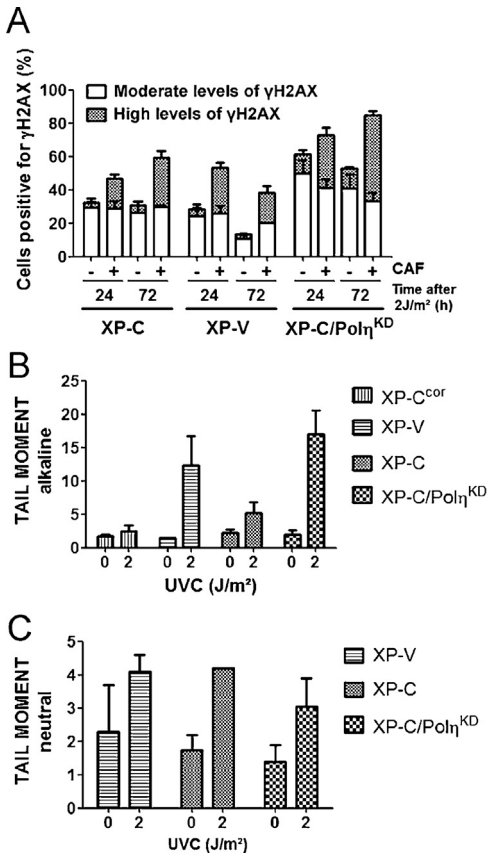

Fig. 7. Caffeine induces high levels of γH2AX and DNA strand breaks in the XPC- and Polη-deficient fibroblasts exposed to a low UVC dose. Cells were treated with 2 J/m^2 UVC in the presence of 1 mM of caffeine (CAF). (A) Percentages of cells positive for γH2AX staining and specifically cells presenting high levels of γH2AX were quantified by flow cytometry. The gates for high levels of γH2AX were defined from the 24 h after 2 J/m^2 UVC time point staining. γH2AX-positive cells, which did not present high levels of this staining, were defined as cells with "moderate levels of γH2AX". (B) DNA strand breaks (single-strand breaks, SSB and double-strand breaks, DSB) and only DSB (C) were detected 24 h after UVC + CAF treatment using the alkaline and neutral comet assay, respectively. Data are presented as means of comet tail moment (±s.e.m.) from at least two experiments performed in triplicate; 100 comets per sample were scored.

pathway [19,23]. In agreement with this hypothesis, CAF attenuated the phosphorylation of Chk1 in XP-C cells irradiated with 2 J/m^2 (Fig. 8A). Thus, the participation of this pathway in UVC-damaged cells was more specifically investigated, by promoting transient ATR KD with siATR. In fact, UVC-induced p-Chk1 levels were decreased in cells transfected with siATR, functionally confirming the silencing of *ATR* gene (Fig. 8B). ATR KD induced an S-phase arrest (data not shown) and an increase in the SubG1 fraction (Fig. 8C) in XP-C, XP-V and XP-C/Polη^{KD} cells exposed to 2 J/m^2. Finally, siATR increased the percentage of UVC-induced γH2AX-positive cells, particularly of cells with high levels of γH2AX (Fig. 8D), in a similar manner to CAF upon UVC (Fig. 7A). Thus, the similarity in the UVC responses of these cells to CAF and ATR KD suggests that the caffeine effect may be mediated by ATR inhibition. Unfortunately, simultaneous treatment with CAF and siATR was toxic to cells in the absence of any additional treatment (Fig. S11), hampering further investigation on this matter.

4. Discussion

Although much is known about how UVC-induced DNA lesions are removed by NER or tolerated by specific TLS polymerases, several questions are still to be answered. For instance, are the different UVC-induced photoproducts bypassed by similar mechanisms and at the same moment of cell cycle? The analysis of the effects of low-dose UVC irradiation in human cells allowed us to observe that unrepaired lesions can be differentially processed by replication machinery, which leads to distinct consequences on cell cycle progression. Indeed, our data indicate that Polη is mainly responsible for lesion bypass during S-phase, leading to a prolonged S-phase arrest in its absence. In its presence, gaps may arise in the newly synthesized strand opposing the UVC damage in the template strand, which are filled independently of replication forks progression.

Quantitative flow cytometry analysis showed that irradiated XP-V fibroblasts were arrested early during replication (Fig. 2C and D) and presented γH2AX staining mainly in the S-phase of the cell cycle (Fig. 3). Although γH2AX is commonly used as double-strand break (DSB) marker, UVC-induced γH2AX in Polη-deficient cells has also been previously associated with the generation of single-stranded DNA (ssDNA) caused by the uncoupling between the replicative DNA polymerase and the helicase at stalled replication forks [23,40,48]. Indeed, we detected single-strand breaks (SSBs), but not DSBs, in XP-V cells (Fig. 4A and B). Also, it has been shown that H2AX is phosphorylated at the vicinity of ssDNA coated with RPA at stalled replication forks [49] and, in fact, not only we showed that the ssDNA-binding protein RPA is recruited to locally irradiated sites presenting γH2AX in XP-V cells (Fig. 4C), but we also detected ssDNA in S/G2-phase cells (Fig. 4D). Considering these results, we hypothesized that in XP-V cells, UVC-induced damage would stall replication forks. Indeed, DNA fiber analyses confirmed a much more pronounced fork elongation arrest in XP-V cells when compared to the control cell line, XP-C^{cor}, or even the XP-C cell line (Fig. 5). Altogether, our observations indicate that γH2AX induced by low-dose of UVC is associated to ssDNA, rather than DSB. Consistent with this, the prolonged stalling of replication forks at UVC damage sites in XP-V cells generated ssDNA. This blockage is probably due to CPDs, as Polη is known to bypass efficiently only this type of photoproduct.

Because most CPDs and 6-4PPs are not repaired in GG-NER-deficient cells, we were surprised to find that low-dose UVC irradiation did not induce early S-phase arrest in XP-C cells as in XP-V cells. Instead, we noticed an accumulation of XP-C cells in G2-phase after 2 J/m^2 and in late S- and G2-phases upon 5 J/m^2 (Fig. 1), suggesting progression of replication forks across UVC damage. Therefore, ssDNA regions (Fig. 4D) and γH2AX formation (Fig. 3) induced by UVC cannot be associated with prolonged replication fork arrest in XP-C cells. Indeed, at 20 min after irradiation, XP-C cells exhibited a more pronounced replication fork stalling, compared to XP-C^{cor} cells, that was overcome at 60 min time point (Fig. 5). Altogether, these data indicate that in XP-C cells the excess of unrepaired UVC damage that initially arrest replication forks are bypassed by a pathway that results in the formation of ssDNA regions, consistent with the gap-filling mechanism of DNA damage tolerance.

Considering that previous work has shown activation of the ATR pathway by ssDNA formed by the uncoupling of the stalled replicative polymerase and helicase [23], we explored whether ssDNA regions which are not associated with prolonged replication forks stalling would have the same effect. Indeed, after low-dose UVC exposure, we detected a similar extent of phosphorylation of the ATR downstream target, Chk1, in XP-V and XP-C cells (Fig. 4E). In UVC-irradiated XP-C cells, ATR activation might be triggered by the accumulation of ssDNA gaps during DNA replication, leading to a mild and temporary G2-phase arrest, in agreement with previous work [18,19,24,50]. Jansen *et al.* reported an irreversible G2-phase arrest in UVC-exposed *Xpc*$^{-/-}$/*Rev1*$^{-/-}$ MEFs [18] which indicates that the resolution of the G2-phase arrest observed may be due to the gap-filling mechanism involving the TLS polymerase Rev1 in

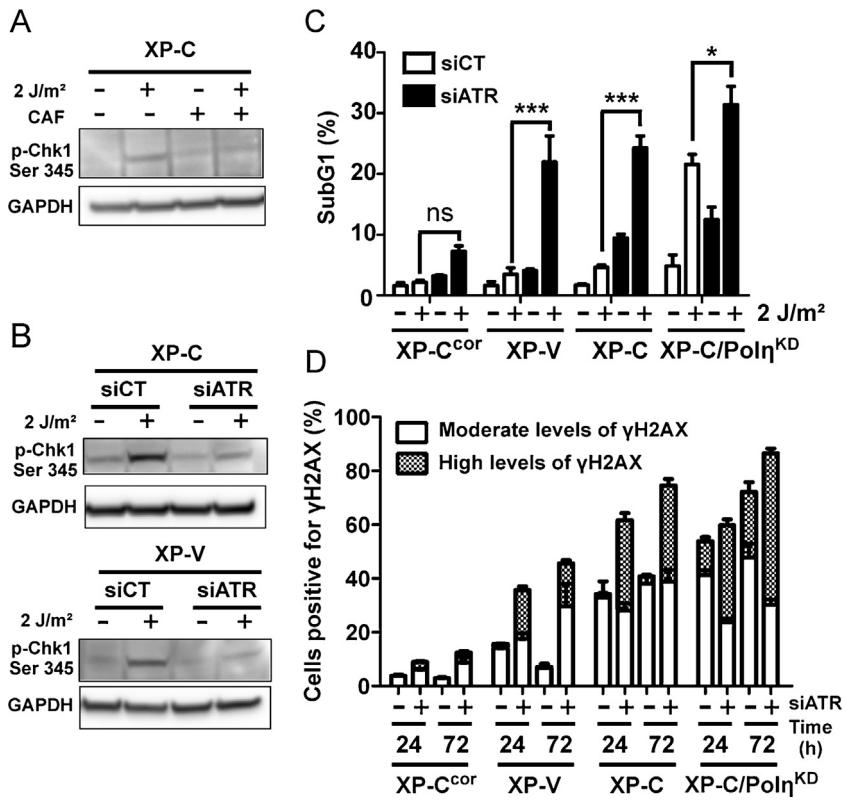

Fig. 8. ATR silencing highly sensitizes XP-V, XP-C and XP-C/Polη^{KD} cells and induces high levels of γH2AX upon low-dose UVC irradiation. Detection of the phosphorylated form of Chk1 (p-Chk1) 6 h after 2 J/m^2 in cells treated with caffeine (CAF) (A) and cells transfected with an siRNA control (siCT) or an siRNA targeting ATR mRNA (siATR) (B). (C) SubG1 fractions were quantified 72 h after 2 J/m^2 in cells transfected with siCT or siATR. Values represent the means (±s.e.m.) of two independent experiments performed in duplicate and the statistical analyses between siCT and siATR for each cell line exposed to UVC were performed with Two-way ANOVA (ns, non significant; $^{*}P < 0.05$; $^{***}P < 0.001$). (D) γH2AX staining was quantified by flow cytometry 24 and 72 h after 2 J/m^2 in cells transfected with siATR (+) or siCT (−). Data represent means (±s.e.m.) of percentages of cells positive for γH2AX staining and specifically cells presenting moderate or high levels of γH2AX from two independent experiments done in duplicate.

this cell cycle phase, also in agreement with other reports [15,24]. However, these authors did not observe any defect in cell cycle progression in UVC-treated *Xpc*$^{-/-}$ MEFs [18] and, to our knowledge, this is the first time that a temporary G2-phase arrest is detected in non-synchronized human cells proficient in TLS exposed to UVC. Interestingly, the presence of unrepaired 6-4PPs is the major difference in terms of lesions in XP-C cells compared to NER-proficient cells, since persistent CPDs can be efficiently bypassed by Polη in GG-NER-deficient cells. Therefore, the different responses between XP-C and XP-V cells observed after UVC irradiation (cell cycle arrest, generation of SSBs and replication fork progression) may indicate that the UVC-DDR observed in XP-C cells is due to the persistence of 6-4PPs rather than CPDs. One possibility is that 6-4PP lesions are mainly bypassed through a post-replicative gap-filling process while CPDs are replicated by Polη directly at the replication fork.

Polη is known to rapidly replicate CPDs, although some data suggest that Polη can also play a role in the bypass of 6-4PPs [26,27]. When the expression of Polη was stably knocked down in XP-C cells, in which most CPDs and 6-4PPs are not repaired, we observed a combined XP-C and XP-V phenotype as inferred from cell cycle arrest in both S- and G2-phases (Fig. 2C and D) and an increase in the γH2AX formation in XP-C/Polη^{KD} cells when compared to XP-C or XP-V cells (Fig. 3). Moreover, in strong contrast with their XP-C counterparts, XP-C/Polη^{KD} cells exhibited SSBs with a higher DNA tailing than the one detected in XP-V cells (Fig. 4A). These results suggest that in the double-deficient cells, besides ssDNA gaps, UVC irradiation also induced prolonged replication fork stalling. Indeed, replication forks elongation was reduced after UVC irradiation in XP-C cells when Polη was depleted (Fig. 5). Surprisingly, at 60 min upon UVC, fork stalling in XP-C/Polη^{KD} cells was apparently less pronounced when compared to XP-V cells. However, the average speed of replication fork progression of the double-deficient cell line is lower than in other cell lines used in this study including XP-V cells (Fig. S6). This suggests that in the XP-C/Polη^{KD} cells the probability of encountering the same amount of DNA lesions within the same time period is reduced.

Taken together, our results may indicate that in XP-C/Polη^{KD} cells there is a superposition of both XP-C and XP-V phenotypes and in this case Polη would not be involved in the gap-filling pathway in irradiated XP-C cells. More precisely, the results can be explained by the fact that in a *XPC*-deficient background, unrepaired CPDs in the genome might block replication forks in the absence of Polη. However, another hypothesis is that because Polη is able to insert the first nucleotide during replication of 6-4PPs with bypass being completed by Polζ [26,27], in Polη-deficient cells, part of unrepaired 6-4PPs could also stall replication forks as CPDs do.

Unlike XP-C and XP-V cells, XP-C/Polη^{KD} cells showed an irreversible cell cycle disruption (Fig. 2C), DSBs (Fig. 4B) and apoptosis induction (Figs. 2E and 6C) after a low UVC dose. Thus, in NER- and Polη-deficient human cells, both ssDNA gaps and prolonged replication forks stalling are generated, although they collapse into DSB, finally leading to cell death.

The UVC-induced phosphorylation of H2AX was related to ATR [40,51], and it is thus intriguing that the inhibition of this kinase by ATR silencing did not abolish the formation of γH2AX, but rather induced an increase in γH2AX formation after UVC irradiation (Fig. 8C). In fact, the increase in γH2AX staining was due to the emergence of a cell population exhibiting high levels of γH2AX in all UVC-irradiated deficient cell lines depleted for ATR but also in XP-C/Polη^{KD} cells exposed to UVC irradiation only (Figs. 3B and 8C).

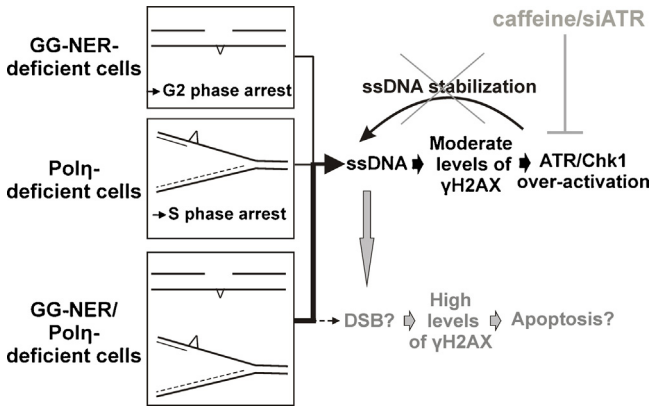

Fig. 9. Model for replicating damaged DNA in GG-NER- and/or Polη-deficient human cells. The black part of the model corresponds to the consequences of UVC irradiation on human fibroblasts while the gray one represents the effects of caffeine or ATR silencing upon UVC exposure. In GG-NER-deficient cells, the replication fork arrest would be resolved by fork restart downstream the lesion. This would generate single-strand DNA (ssDNA) gaps during and after DNA replication. In Polη-deficient cells, replication fork stalling would be prolonged and therefore the uncoupling between the replicative polymerase and the helicase would also lead to the formation of ssDNA region. In cells deficient in both NER and Polη, both ssDNA gaps and ssDNA due to replicative polymerase stalling would be induced at the same time by UVC irradiation and thus there would be a more important amount of ssDNA regions in these double-deficient cells than in both single-deficient cell lines (represented by the thick arrow). In either case, the induction of ssDNA would lead to Ser139 H2AX phosphorylation, generating moderate levels of γH2AX. According to a recent work, the formation of γH2AX mediates ATR/Chk1 pathway over-activation [49], which in turn, may stabilize ssDNA and induce cell cycle arrest. In the case of ssDNA gaps, this checkpoint activation may lead to a G2-phase arrest while stalled replication forks would induce intra-S-phase arrest. ATR inhibition (by CAF or ATR silencing) could induce double-strand breaks (DSB) in UVC-exposed cells as a consequence of the collapse of ssDNA structures. In this case, another kinase than ATR could phosphorylate H2AX, leading to high levels of γH2AX. In this scenario, UVC-induced DSB would mainly conduct cells to death. Strikingly, the presence of unresolved ssDNA structures in GG-NER/Polη-deficient cells may lead to collapse into DSB, represented by the dotted line.

These results show that the generation of high levels of γH2AX is independent of the ATR kinase. Interestingly, similar results were obtained with cells co-treated with CAF and UVC (Fig. 7A and S8), underscoring that the effect of CAF in UVC-exposed cells might be mainly associated with the inhibition of ATR/Chk1. This is in agreement with previous reports [19,23,47,52,53] and in line with the observation that CAF abolishes the activation of Chk1 upon low-dose UVC treatment (Fig. 8A). Intriguingly, we detected low levels of DSB by the neutral comet assay in XP-C and XP-V cells co-treated with CAF and UVC and in irradiated XP-C/Polη^{KD} both treated or not with CAF (Figs. 4B and 7C), which correlates to the emergence of high levels of γH2AX (Fig. 7A) mainly in S- and G2-phases (Fig. 3B and S7), therefore suggesting that only cells with high levels of γH2AX actually present DSBs. Moreover, we also observed a strong correlation between DSB formation and apoptosis induction (compare Figs. 4B, 6B, 6C and 7C). It has been shown that co-treatment with CAF and UVC redirect S-phase cells into an apoptotic pathway [43,47,54,55]. Therefore, it is likely that CAF and UVC-exposed S/G2-phases cells switched to a DSB pathway inducing intense γH2AX staining [43], represented here by the high levels of γH2AX. These results indicate that for XP-C and XP-V cells co-treated with CAF and UVC irradiation, DSBs are generated from the collapse of ssDNA structures that are no longer stabilized by the ATR pathway, leading to cell death. For XP-C/Polη^{KD} cells, UVC-induced ssDNA replicative intermediates collapse directly into DSBs even in the absence of ATR inhibition, increasing the sensitivity of these cells to UVC irradiation.

In conclusion, based on the results presented herein and those previously published elsewhere, we propose a model in which both damage tolerance at the replication fork and post-replicative gap-filling bypass mechanism play an essential role in the recovery of human cells after UVC exposure. In this model (Fig. 9), ssDNA gaps are generated in the genome of human XP-C cells, which allow cells to go through S-phase and arrest in G2-phase. These gaps would then be filled independently of DNA replication, thus resolving the cell cycle arrest. In contrast, XP-V cells accumulate in S-phase due to the blockage of fork progression by DNA damage. The ssDNA formed in both cell types result in signaling for H2AX phosphorylation. In cells deficient in GG-NER and Polη, both ssDNA replicative intermediates (replication fork blockage and ssDNA gaps) are generated and part of these structures collapse into DSBs, resulting in the formation of high levels of γH2AX and cell death. ATR inhibition exacerbates these effects, underscoring the role of checkpoint activation in the stabilization of both replication intermediates. The possibility that CPDs and 6-4PPs are responsible for the different responses in XP-V (prolonged blockage of fork progression) or XP-C (ssDNA gaps) cells, respectively, is currently under investigation. Although the effects observed in this work were certainly strengthened by the lack of a functional G1/S checkpoint and DNA repair defects, these processes probably reflect the consequences of a small number of lesions in human cells and disclose the involvement of DNA damage tolerance at the replication fork and also after replication fork restart. The establishment of a stable XP-C/Polη^{KD} human cell line has paved the way to further investigations regarding the role of Polη in the bypass of 6-4PPs in the human genome.

Conflict of interest statement

The authors declare that there are no conflicts of interest.

Acknowledgements

The authors thank Leonardo C. Andrade-Lima for indications for siRNA and active Caspase 3 experiments, the Fundação de Amparo à Pesquisa do Estado de São Paulo (FAPESP, São Paulo, Brazil); Conselho Nacional de Desenvolvimento Científico e Tecnológico (CNPq, Brasília, DF, Brazil); Coordenação de Aperfeiçoamento de Pessoal de Nível Superior (CAPES, Brasília, DF, Brazil); Centre National de Recherche Scientifique (CNRS, France), Association Française des Myopathies (Evry, France), Association Française des Enfants de la Lune (Tercis, France) and ANPCyT (Argentina) for Grant support. ATV and CRRR had a fellowship from FAPESP and AQ had a fellowship from French government (Ministère de l'Enseignement Supérieur et de la Recherche).

Appendix A. Supplementary data

Supplementary data associated with this article can be found, in the online version, at http://dx.doi.org/10.1016/j.dnarep.2013.12.005.

References

[1] J. Hoeijmakers, Genome maintenance mechanisms for preventing cancer, Nature 411 (2001) 366–374.
[2] J.E. Cleaver, Cancer in xeroderma pigmentosum and related disorders of DNA repair, Nat. Rev. Cancer 5 (2005) 564–573.
[3] R. Costa, V. Chiganças, R.S. Galhardo, H. Carvalho, C. Menck, The eukaryotic nucleotide excision repair pathway, Biochimie 85 (2003) 1083–1099.
[4] P.C. Hanawalt, Subpathways of nucleotide excision repair and their regulation, Oncogene 21 (2002) 8949–8956.
[5] S. Tornaletti, G. Pfeifer, UV damage and repair mechanisms in mammalian cells, Bioessays 18 (1996) 221–228.
[6] L. Riou, L. Zeng, O. Chevallier-Lagente, A. Stary, O. Nikaido, A. Taïeb, G. Weeda, M. Mezzina, A. Sarasin, The relative expression of mutated XPB genes results in xeroderma pigmentosum/Cockayne's syndrome or trichothiodystrophy cellular phenotypes, Hum. Mol. Genet. 8 (1999) 1125–1133.

[7] J.E. Sale, A.R. Lehmann, R. Woodgate, Y-family DNA polymerases and their role in tolerance of cellular DNA damage, Nat. Rev. Mol. Cell Biol. 13 (2012) 141–152.
[8] A.R. Lehmann, R.P. Fuchs, Gaps and forks in DNA replication: rediscovering old models, DNA Repair (Amst) 5 (2006) 1495–1498.
[9] C.E. Edmunds, L.J. Simpson, J.E. Sale, PCNA ubiquitination and REV1 define temporally distinct mechanisms for controlling translesion synthesis in the avian cell line DT40, Mol. Cell 30 (2008) 519–529.
[10] J.G. Jansen, M.I. Fousteri, N. de Wind, Send in the clamps: control of DNA translesion synthesis in eukaryotes, Mol. Cell 28 (2007) 522–529.
[11] A.R. Lehmann, S. Kirk-Bell, C.F. Arlett, M.C. Paterson, P.H. Lohman, E.A. de Weerd-Kastelein, D. Bootsma, Xeroderma pigmentosum cells with normal levels of excision repair have a defect in DNA synthesis after UV-irradiation, Proc. Natl. Acad. Sci. U S A 72 (1975) 219–223.
[12] M. Lopes, M. Foiani, J.M. Sogo, Multiple mechanisms control chromosome integrity after replication fork uncoupling and restart at irreparable UV lesions, Mol. Cell 21 (2006) 15–27.
[13] R. Meneghini, Gaps in DNA synthesized by ultraviolet light-irradiated WI38 human cells, Biochim. Biophys. Acta 425 (1976) 419–427.
[14] Y. Daigaku, A.A. Davies, H.D. Ulrich, Ubiquitin-dependent DNA damage bypass is separable from genome replication, Nature 465 (2010), 951-U913.
[15] N. Diamant, A. Hendel, I. Vered, T. Carell, T. Reissner, N. de Wind, N. Geacinov, Z. Livneh, DNA damage bypass operates in the S and G2 phases of the cell cycle and exhibits differential mutagenicity, Nucleic Acids Res. 40 (2012) 170–180.
[16] G.I. Karras, S. Jentsch, The RAD6 DNA damage tolerance pathway operates uncoupled from the replication fork and is functional beyond S phase, Cell 141 (2010) 255–267.
[17] A.J. Callegari, E. Clark, A. Pneuman, T.J. Kelly, Postreplication gaps at UV lesions are signals for checkpoint activation, Proc. Natl. Acad. Sci. U S A 107 (2010) 8219–8224.
[18] J.G. Jansen, A. Tsaalbi-Shtylik, G. Hendriks, H. Gali, A. Hendel, F. Johansson, K. Erixon, Z. Livneh, L.H. Mullenders, L. Haracska, N. de Wind, Separate domains of Rev1 mediate two modes of DNA damage bypass in mammalian cells, Mol. Cell Biol. 29 (2009) 3113–3123.
[19] M. Wigan, A. Pinder, N. Giles, S. Pavey, A. Burgess, S. Wong, R.A. Sturm, B. Gabrielli, A UVR-induced G2-phase checkpoint response to ssDNA gaps produced by replication fork bypass of unrepaired lesions is defective in melanoma, J. Invest. Dermatol. 132 (2012) 1681–1688.
[20] S.S. Lange, K. Takata, R.D. Wood, DNA polymerases and cancer, Nat. Rev. Cancer 11 (2011) 96–110.
[21] C. Masutani, R. Kusumoto, S. Iwai, F. Hanaoka, Mechanisms of accurate translesion synthesis by human DNA polymerase eta, EMBO J. 19 (2000) 3100–3109.
[22] A.M. Cordonnier, R.P. Fuchs, Replication of damaged DNA: molecular defect in xeroderma pigmentosum variant cells, Mutat. Res. 435 (1999) 111–119.
[23] E. Despras, F. Daboussi, O. Hyrien, K. Marheineke, P.L. Kannouche, ATR/Chk1 pathway is essential for resumption of DNA synthesis and cell survival in UV-irradiated XP variant cells, Hum. Mol. Genet. 19 (2010) 1690–1701.
[24] P. Temviriyanukul, S. van Hees-Stuivenberg, F. Delbos, H. Jacobs, N. de Wind, J.G. Jansen, Temporally distinct translesion synthesis pathways for ultraviolet light-induced photoproducts in the mammalian genome, DNA Repair (Amst) 11 (2012) 550–558.
[25] I. Elvers, F. Johansson, P. Groth, K. Erixon, T. Helleday, UV stalled replication forks restart by re-priming in human fibroblasts, Nucleic Acids Res. 39 (2011) 7049–7057.
[26] J.H. Yoon, L. Prakash, S. Prakash, Error-free replicative bypass of (6-4) photoproducts by DNA polymerase zeta in mouse and human cells, Genes Dev. 24 (2010) 123–128.
[27] A. Bresson, R.P. Fuchs, Lesion bypass in yeast cells: Pol eta participates in a multi-DNA polymerase process, EMBO J. 21 (2002) 3881–3887.
[28] D. Huang, B.D. Piening, A.G. Paulovich, The preference for error-free or error-prone postreplication repair in *Saccharomyces cerevisiae* exposed to low-dose methyl methanesulfonate is cell cycle dependent, Mol. Cell Biol. 33 (2013) 1515–1527.
[29] D.S. Biard, Untangling the relationships between DNA repair pathways by silencing more than 20 DNA repair genes in human stable clones, Nucleic Acids Res. 35 (2007) 3535–3550.
[30] L. Rey, J.M. Sidorova, N. Puget, F. Boudsocq, D.S. Biard, R.J. Monnat, C. Cazaux, J.S. Hoffmann, Human DNA polymerase eta is required for common fragile site stability during unperturbed DNA replication, Mol. Cell Biol. 29 (2009) 3344–3354.
[31] R. Bétous, L. Rey, G. Wang, M.J. Pillaire, N. Puget, J. Selves, D.S. Biard, K. Shin-ya, K.M. Vasquez, C. Cazaux, J.S. Hoffmann, Role of TLS DNA polymerases eta and kappa in processing naturally occurring structured DNA in human cells, Mol. Carcinog. 48 (2009) 369–378.
[32] S. Koundrioukoff, S. Carignon, H. Técher, A. Letessier, O. Brison, M. Debatisse, Stepwise activation of the ATR signaling pathway upon increasing replication stress impacts fragile site integrity, PLoS Genet. 9 (2013) e1003643.
[33] M.C. Moraes, A.Q. de Andrade, H. Carvalho, T. Guecheva, M.H. Agnoletto, J.A. Henriques, A. Sarasin, A. Stary, J. Saffi, C.F. Menck, Both XPA and DNA polymerase eta are necessary for the repair of doxorubicin-induced DNA lesions, Cancer Lett. 314 (2012) 108–118.
[34] J. Saffi, M.H. Agnoletto, T.N. Guecheva, L.F. Batista, H. Carvalho, J.A. Henriques, A. Stary, C.F. Menck, A. Sarasin, Effect of the anti-neoplastic drug doxorubicin on XPD-mutated DNA repair-deficient human cells, DNA Repair (Amst) 9 (2010) 40–47.
[35] J. Speroni, M.B. Federico, S.F. Mansilla, G. Soria, V. Gottifredi, Kinase-independent function of checkpoint kinase 1 (Chk1) in the replication of damaged DNA, Proc. Natl. Acad. Sci. U S A 109 (2012) 7344–7349.
[36] D. Biard, E. Despras, A. Sarasin, J. Angulo, Development of new EBV-based vectors for stable expression of small interfering RNA to mimick human syndromes: application to NER gene silencing, Mol. Cancer Res. 3 (2005) 519–529.
[37] C.F. Arlett, S.A. Harcourt, B.C. Broughton, The influence of caffeine on cell survival in excision-proficient and excision-deficient xeroderma pigmentosum and normal human cell strains following ultraviolet-light irradiation, Mutat. Res. 33 (1975) 341–346.
[38] E. Rogakou, D. Pilch, A. Orr, V. Ivanova, W. Bonner, DNA double-stranded breaks induce histone H2AX phosphorylation on serine 139, J. Biol. Chem. 273 (1998) 5858–5868.
[39] M.G. Vrouwe, A. Pines, R.M. Overmeer, K. Hanada, L.H. Mullenders, UV-induced photolesions elicit ATR-kinase-dependent signaling in non-cycling cells through nucleotide excision repair-dependent and -independent pathways, J. Cell Sci. 124 (2011) 435–446.
[40] I. Ward, J. Chen, Histone H2AX is phosphorylated in an ATR-dependent manner in response to replicational stress, J. Biol. Chem. 276 (2001) 47759–47762.
[41] C. Limoli, E. Giedzinski, W. Bonner, J. Cleaver, UV-induced replication arrest in the xeroderma pigmentosum variant leads to DNA double-strand breaks, gamma-H2AX formation, and Mre11 relocalization, Proc. Natl. Acad. Sci. U S A 99 (2002) 233–238.
[42] T. Marti, E. Hefner, L. Feeney, V. Natale, J. Cleaver, H2AX phosphorylation within the G1 phase after UV irradiation depends on nucleotide excision repair and not DNA double-strand breaks, Proc. Natl. Acad. Sci. U S A 103 (2006) 9891–9896.
[43] J.E. Cleaver, L. Feeney, I. Revet, Phosphorylated H2Ax is not an unambiguous marker for DNA double-strand breaks, Cell Cycle 10 (2011) 3223–3224.
[44] C. Godon, S. Mourgues, J. Nonnekens, A. Mourcet, F. Coin, W. Vermeulen, P.O. Mari, G. Giglia-Mari, Generation of DNA single-strand displacement by compromised nucleotide excision repair, EMBO J. 31 (2012) 3550–3563.
[45] Y. Yang, M. Durando, S.L. Smith-Roe, C. Sproul, A.M. Greenwalt, W. Kaufmann, S. Oh, E.A. Hendrickson, C. Vaziri, Cell cycle stage-specific roles of Rad18 in tolerance and repair of oxidative DNA damage, Nucleic Acids Res. 41 (2013) 2296–2312.
[46] N. Bendris, B. Lemmers, J.M. Blanchard, N. Arsic, Cyclin A2 mutagenesis analysis: a new insight into CDK activation and cellular localization requirements, PLoS One 6 (2011) e22879.
[47] S. de Feraudy, I. Revet, V. Bezrookove, L. Feeney, J.E. Cleaver, A minority of foci or pan-nuclear apoptotic staining of gammaH2AX in the S phase after UV damage contain DNA double-strand breaks, Proc. Natl. Acad. Sci. U S A 107 (2010) 6870–6875.
[48] D.J. Chang, P.J. Lupardus, K.A. Cimprich, Monoubiquitination of proliferating cell nuclear antigen induced by stalled replication requires uncoupling of DNA polymerase and mini-chromosome maintenance helicase activities, J. Biol. Chem. 281 (2006) 32081–32088.
[49] J. Wang, Z. Gong, J. Chen, MDC1 collaborates with TopBP1 in DNA replication checkpoint control, J. Cell Biol. 193 (2011) 267–273.
[50] S. Yan, W.M. Michael, TopBP1 and DNA polymerase alpha-mediated recruitment of the 9-1-1 complex to stalled replication forks: implications for a replication restart-based mechanism for ATR checkpoint activation, Cell Cycle 8 (2009) 2877–2884.
[51] M. Matsumoto, K. Yaginuma, A. Igarashi, M. Imura, M. Hasegawa, K. Iwabuchi, T. Date, T. Mori, K. Ishizaki, K. Yamashita, M. Inobe, T. Matsunaga, Perturbed gap-filling synthesis in nucleotide excision repair causes histone H2AX phosphorylation in human quiescent cells, J. Cell Sci. 120 (2007) 1104–1112.
[52] I. Elvers, A. Hagenkort, F. Johansson, T. Djureinovic, A. Lagerqvist, N. Schultz, I. Stoimenov, K. Erixon, T. Helleday, CHK1 activity is required for continuous replication fork elongation but not stabilization of post-replicative gaps after UV irradiation, Nucleic Acids Res. 40 (2012) 8440–8448.
[53] T.P. Heffernan, M. Kawasumi, A. Blasina, K. Anderes, A.H. Conney, P. Nghiem, ATR-Chk1 pathway inhibition promotes apoptosis after UV treatment in primary human keratinocytes: potential basis for the UV protective effects of caffeine, J. Invest. Dermatol. 129 (2009) 1805–1815.
[54] H. Halicka, X. Huang, F. Traganos, M. King, W. Dai, Z. Darzynkiewicz, Histone H2AX phosphorylation after cell irradiation with UV-B: relationship to cell cycle phase and induction of apoptosis, Cell Cycle 4 (2005) 339–345.
[55] J.E. Cleaver, γH2Ax: biomarker of damage or functional participant in DNA repair "all that glitters is not gold!", Photochem. Photobiol. 87 (2011) 1230–1239.